Int. J. Anal. Appl. (2026), 24:109

International Journal of Analysis and Applications

Sombor Indices and Entropy Measures of Tetrahedral Diamond Lattices: Analytical and Graphical Insights

Mariadhas Kavitha, Sathish Krishnan*

Department of Mathematics and Statistics, Faculty of Science and Humanities, SRM Institute of Science and Technology, Chengalpattu, 603203, India

**Corresponding author:* sathishk6@srmist.edu.in

Abstract. The crystal form of a diamond is a face-centered lattice. The atoms in diamonds are arranged in a diamond cubic crystal structure. Each carbon atom in a diamond is surrounded by four other carbon atoms that are joined by covalent bonds. Topological indices are widely employed to present molecular characteristics in cheminformatics. In QSAR/QSPR study, topological indices are utilized to predict the bioactivity of chemical compounds. For determining the structural information of molecular graphs and complex networks, graph entropies with topological indices are used. The graph entropy measures play an important role in a variety of problem areas including, discrete mathematics, biology, and chemistry. In this paper the exact analytical expressions for Sombor indices and their entropy measures for the graph of tetrahedral diamond lattices are computed.

1. Introduction

Mathematics, chemistry, and information science are combined in a recently emerged field termed cheminformatics. Chemical graphs, in which the atoms are the vertices and the molecular bonds are the edges, can be used to represent chemical systems. Molecular graphs are a unique kind of chemical graphs that depict the structure of molecules. Topological indices are employed in theoretical chemistry to investigate quantitative structure-property relations (QSPR) and quantitative structure-activity relations (QSAR). The structures of chemical compounds are described by topological indices, which are molecular descriptors that can be utilized for predicting physicochemical properties like stability, enthalpy of vaporization, boiling point, and so on. Numerous topological indices associated with degree, distance, or counting exist. Among them, degree-based topological indices are known to be useful tools for chemical studies. Topological indices have

Received: Nov. 2, 2025.

2020 *Mathematics Subject Classification.* 05C09, 05C92.

Key words and phrases. molecular graph; topological indices; Sombor indices; entropy measures; tetrahedral diamond lattice.

https://doi.org/10.28924/2291-8639-24-2026-109
© 2026 the author(s).
ISSN: 2291-8639

many applications in risk assessment, toxicity prediction, regularity decisions, drug discovery and lead optimization ([3], [4], [5], [7]).

Let $G = (V, E)$ be a molecular graph with vertex set $V(G)$ and edge set $E(G)$. For an edge uv, we call u and v the end vertices of uv. For a vertex $x \in V(G)$, the open neighborhood of x is the set $N(x) = \{y \in V(G) : xy \in E(G)\}$, and the closed neighborhood of x is $N[x] = N(x) \cup \{x\}$. The degree of a vertex $x \in V(G)$, denoted by $deg(x)$, is $\mid N(x) \mid$.

One of the oldest degree-based topological index is the first Zagreb index which was introduced in 1972 and defined [3] as follows:

$$M_1(G) = \sum_{v \in V} deg(v)^2 \tag{1.1}$$

This measure was developed in the process of examining how molecular structure depends on pi-electron energy. This index has gained a lot of attention since it was first introduced, particularly from mathematicians. A new graph invariant called the Sombor index based on vertex degree was recently proposed [6] and defined as

$$SO(G) = \sum_{uv \in E} \sqrt{deg(u)^2 + deg(v)^2} \tag{1.2}$$

Recently other versions of Sombor index are also introduced [8,10] and defined as follows:

$$SO_{red}(G) = \sum_{uv \in E} \sqrt{(deg(u) - 1)^2 + (deg(v) - 1)^2} \tag{1.3}$$

$$SO_{avg}(G) = \sum_{uv \in E} \sqrt{\left(deg(u) - \frac{2m}{n}\right)^2 + \left(deg(v) - \frac{2m}{n}\right)^2} \tag{1.4}$$

$${}^{m}SO(G) = \sum_{uv \in E} \frac{1}{\sqrt{deg(u)^2 + deg(v)^2}} \tag{1.5}$$

$$SO_3(G) = \sum_{uv \in E} \sqrt{2}\pi \left(\frac{deg(u)^2 + deg(v)^2}{deg(u) + deg(v)}\right) \tag{1.6}$$

$$SO_4(G) = \sum_{uv \in E} \frac{\pi}{2} \left(\frac{deg(u)^2 + deg(v)^2}{deg(u) + deg(v)}\right)^2 \tag{1.7}$$

A crucial quantity in information theory is the graph entropy. Graph entropy measures have also found extensive use in computer science, structural chemistry, and biology [2]. The idea of entropy was initiated by Shannon in 1948 [12]. In 2014, Chen et al. [1] proposed the definition of entropy of an edge-weighted graph G. Let $G = (V, E, \Psi(u_i v_j))$ be an edge-weighted graph, where V, E and $\Psi(u_i v_j)$ exemplify the set of vertices, the edge set, and the edge weight of edge $(u_i v_j)$, respectively. The entropy of edge weighted graph is defined as

$$ENT_{\Psi(G)} = \sum_{u_i v_j \in E} \frac{\Psi(u_i v_j)}{\sum\limits_{u_i v_j \in E} \Psi(u_i v_j)} log\left[\frac{\Psi(u_i v_j)}{\sum\limits_{u_i v_j \in E} \Psi(u_i v_j)}\right] \tag{1.8}$$

Recently the concept of entropies measures of Sombor indices was introduced [11] and defined as follows:

$$ENT_{SO} = log(SO(G)) - \frac{1}{SO(G)} log\left[\prod_{uv\in E} \alpha^{\alpha}\right] \tag{1.9}$$

where $\alpha = \sqrt{deg(u)^2 + deg(v)^2}$

$$ENT_{SO_{red}} = log(SO_{red}(G)) - \frac{1}{SO_{red}(G)} log\left[\prod_{uv\in E} \beta^{\beta}\right] \tag{1.10}$$

where $\beta = \sqrt{(deg(u)-1)^2 + (deg(v)-1)^2}$

$$ENT_{SO_{avr}} = log(SO_{avr}(G)) - \frac{1}{SO_{avr}(G)} log\left[\prod_{uv\in E} \gamma^{\gamma}\right] \tag{1.11}$$

where $\gamma = \sqrt{\left(deg(u) - \frac{2m}{n}\right)^2 + \left(deg(v) - \frac{2m}{n}\right)^2}$

$$ENT_{^mSO} = log(^mSO(G)) - \frac{1}{^mSO(G)} log\left[\prod_{uv\in E} \zeta^{\zeta}\right] \tag{1.12}$$

where $\zeta = \frac{1}{\sqrt{deg(u)^2+deg(v)^2}}$

$$ENT_{SO_3} = log(SO_3(G)) - \frac{1}{SO_3(G)} log\left[\prod_{uv\in E} \eta^{\eta}\right] \tag{1.13}$$

where $\eta = \sqrt{2}\pi\left(\frac{deg(u)^2+deg(v)^2}{deg(u)+deg(v)}\right)$

$$ENT_{SO_4} = log(SO_4(G)) - \frac{1}{SO_4(G)} log\left[\prod_{uv\in E} \theta^{\theta}\right] \tag{1.14}$$

where $\theta = \frac{\pi}{2}\left(\frac{deg(u)^2+deg(v)^2}{deg(u)+deg(v)}\right)^2$

In this paper the exact analytical expressions for Sombor indices and their entropy measures for the graph of tetrahedral diamond lattices are computed.

2. Tetrahedral Diamond Lattice

Among the constituents of the chemical system, carbon is the most notable and significant. The carbon atom creates a wide range of compounds because of its comparatively small size and strong single, double, and triple chemical bonding capabilities with other small atoms and carbon atoms. The vast majority of chemical compounds roughly ten million in total are carbon-based. For several decades, the materials science community has been captivated by carbon-based materials. Graphite, diamond, and amorphous carbon are well-known classic examples of carbon allotropes.

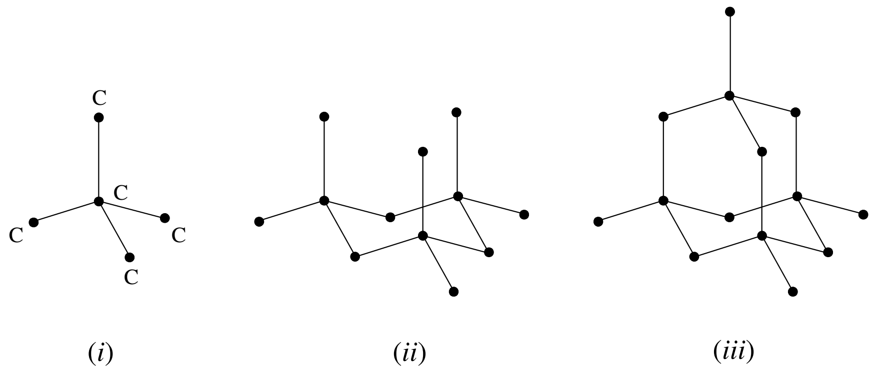

Figure 1. (*i*) Tetrahedral arrangement of carbon atoms (*ii*) Puckered hexagonal ring (*iii*) Unit cell

A diamond is simply an extended structure of carbon atoms with sp^3 bonds that are tetrahedrally coordinated. The diamond is recognized for its exceptional material hardness due to the incompressibility of its C-C bonds and the three-dimensional stability of the tetrahedral bonding structure. Diamond is a material with considerable potential for usage in numerous industrial and commercial applications due to its various extreme qualities. Among these are the following: diamond is used for heat spreaders, lining hip joints, surgical blades, radiation detectors, glass grinding, metal cutting, wire drawing, oil and gas drilling, stone and wood sawing, wear-resistant coatings, polishing other materials, and even for enhancing golf club driving performance.

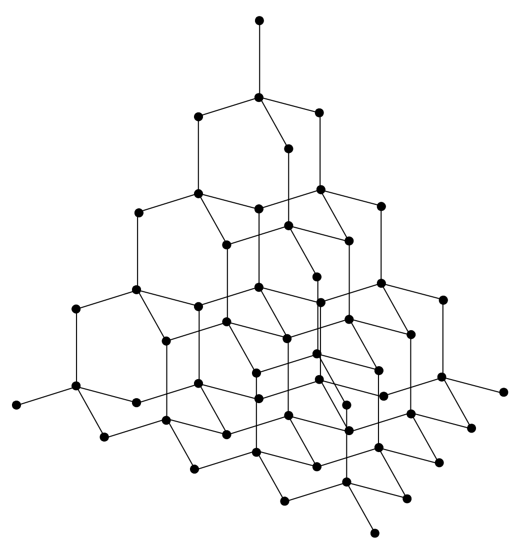

Figure 2. Tetrahedral diamond lattice

As shown in Figure 1 (*i*), each carbon atom in the diamond structure is attached to four other carbon atoms in a tetrahedral arrangement. Three tetrahedral arrangements of carbon atoms are joined together to form a puckered hexagonal ring as in Figure 1 (*ii*). This puckered hexagonal ring is capped by a fourth tetrahedral to form a structure that preserves the tetrahedral arrangement as in Figure 1 (*iii*). By repeatedly employing this building block, we get a larger structure which retains the tetrahedral structure as depicted in Figure 2 [9]. Let $TD(n)$ be the graph of tetrahedral diamond lattice of dimension n with n layers. Figure 3 depicts different layers of a tetrahedral diamond lattice $TD(5)$.

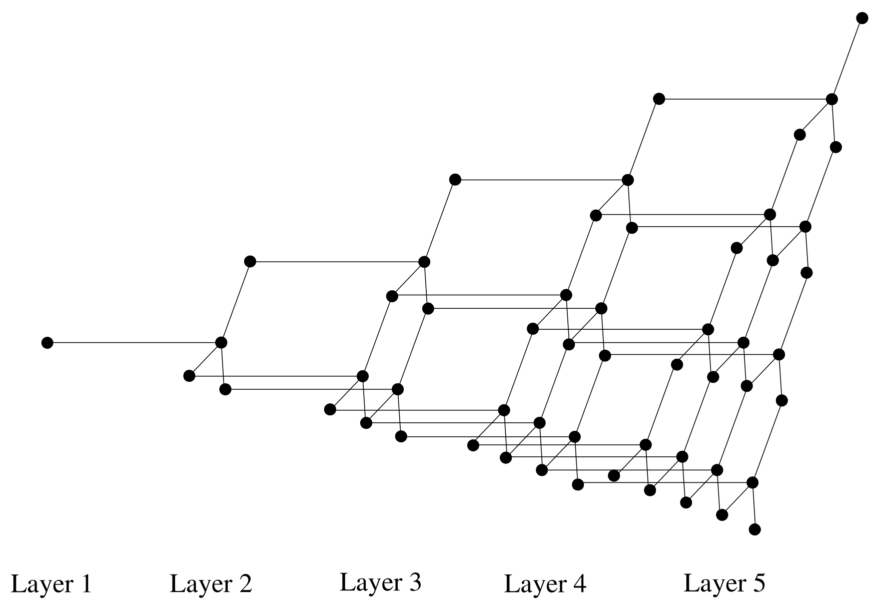

Figure 3. Different layers of a tetrahedral diamond lattice

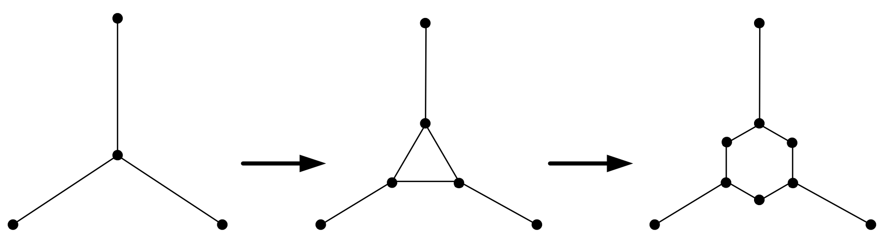

Figure 4. Construction of Layer 3 from Layer 2

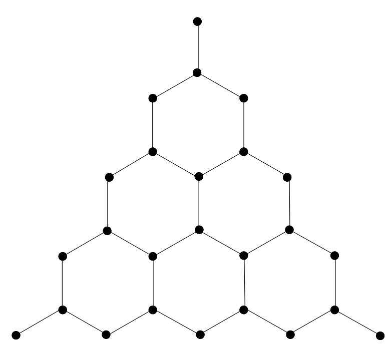

Figure 5. Graph of Layer 5

Table 1. The edge partition of G based on the degrees of end vertices of each edge

$(deg(u), deg(v))$ where $uv \in E$	Number of edges
$(1,4)$	4
$(2,4)$	$12(n-2)$
$(3,4)$	$6n^2-30n+36$
$(4,4)$	$\frac{1}{3}(2n^3-18n^2+52n-48)$

2.1. **Construction of layers of tetrahedral diamond lattice.** Layer 1 is just a single vertex. Layer 2 is isomorphic to $K_{1,3}$. To construct Layer 3 from Layer 2, replace the 3-degree vertex of Layer 2 by K_3, a complete graph on three vertices, and subdivide each edge of K_3. See Figure 4. To construct Layer k, $4 \le k \le n$, arrange regular hexagons in $k-2$ rows in the form of equilateral triangle such that the first row has one hexagon, second row has two hexagons and so on and the $(k-2)$th row has $k-2$ hexagons. Include three pendant edges to the graph constructed as shown in Figure 5. The vertices and edges included are treated as the vertices and edges of layer k. It is clear that each layer k, $3 \le k \le n$, is made up of $\frac{(k-1)(k-2)}{2}$ hexagons with three pendent edges. See Figure 3.

Theorem 2.1. *Let G be $TD(n)$. Then the number of vertices and edges of G are $\frac{n(n+1)(2n+1)}{6}$ and $\frac{2n(n^2-1)}{3}$ respectively.*

3. Main Results

Theorem 3.1. *Let G be tetrahedral diamond lattice $TD(n), n \ge 4$. Then*

(1) $SO(G) = \frac{1}{3}[8\sqrt{2}n^3 + (90-72\sqrt{2})n^2 + (208\sqrt{2}+72\sqrt{5}-450)n + (540+12\sqrt{17}-192\sqrt{2}-144\sqrt{5})]$

(2) $SO_{red}(G) = 2\sqrt{2}n^3 + (6\sqrt{13}-18\sqrt{2})n^2 - (30\sqrt{13}-52\sqrt{2}-12\sqrt{10})n + (36\sqrt{13}-48\sqrt{2}-24\sqrt{10}+12)$

(3) $SO_{avr}(G) = \frac{1}{(2n+1)}\Big[4\sqrt{36n^2-108n+225} + 24(n-2)\sqrt{4n^2-20n+61} + (6n^2-30n+36)\sqrt{4n^2-44n+265} + 4\sqrt{2}(2n^3-18n^2+52n-48)\Big]$

(4) ${}^{m}SO(G) = \frac{1}{6\sqrt{2}}n^3 + \left(\frac{6}{5} - \frac{3}{2\sqrt{2}}\right)n^2 + \left(\frac{6}{\sqrt{5}} - 6 + \frac{13}{3\sqrt{2}}\right)n + \left(\frac{4}{\sqrt{17}} - \frac{12}{\sqrt{5}} + \frac{36}{5} - \frac{4}{\sqrt{2}}\right)$

(5) $SO_3(G) = \frac{\sqrt{2}\pi}{105}[280n^3 - 270n^2 + 230n - 192]$

(6) $SO_4(G) = \frac{\pi}{7350}[39200n^3 - 71550n^2 + 102950n - 63368]$

Proof. Consider the graph G. When Table 1 is used with equations 1.2–1.7, we get

$$SO(G) = 4\sqrt{1^2+4^2} + 12(n-2)\sqrt{2^2+4^2} + (6n^2-30n+36)\sqrt{3^2+4^2} + \frac{1}{3}(2n^3-18n^2+52n-48)\sqrt{4^2+4^2}$$
$$= \frac{1}{3}[8\sqrt{2}n^3 + (90-72\sqrt{2})n^2 + (208\sqrt{2}+72\sqrt{5}-450)n + (540+12\sqrt{17}-192\sqrt{2}-144\sqrt{5})]$$

$$SO_{red}(G) = 4\sqrt{(1-1)^2+(4-1)^2} + 12(n-2)\sqrt{(2-1)^2+(4-1)^2} + (6n^2-30n+36)\sqrt{(3-1)^2+(4-1)^2}$$
$$+ \frac{1}{3}(2n^3-18n^2+52n-48)\sqrt{(4-1)^2+(4-1)^2}$$
$$= 2\sqrt{2}n^3 + (6\sqrt{13}-18\sqrt{2})n^2 - (30\sqrt{13}-52\sqrt{2}-12\sqrt{10})n + (36\sqrt{13}-48\sqrt{2}-24\sqrt{10}+12)$$

$$SO_{avr}(G) = 4\sqrt{\left(1-\frac{8(n^2-1)}{(n+1)(2n+1)}\right)^2 + \left(4-\frac{8(n^2-1)}{(n+1)(2n+1)}\right)^2}$$
$$+ 12(n-2)\sqrt{\left(2-\frac{8(n^2-1)}{(n+1)(2n+1)}\right)^2 + \left(4-\frac{8(n^2-1)}{(n+1)(2n+1)}\right)^2}$$
$$+ (6n^2-30n+36)\sqrt{\left(3-\frac{8(n^2-1)}{(n+1)(2n+1)}\right)^2 + \left(4-\frac{8(n^2-1)}{(n+1)(2n+1)}\right)^2}$$
$$+ \frac{1}{3}(2n^3-18n^2+52n-48)\sqrt{\left(4-\frac{8(n^2-1)}{(n+1)(2n+1)}\right)^2 + \left(4-\frac{8(n^2-1)}{(n+1)(2n+1)}\right)^2}$$
$$= \frac{1}{(2n+1)}\Big[4\sqrt{36n^2-108n+225} + 24(n-2)\sqrt{4n^2-20n+61} + (6n^2-30n+36)\sqrt{4n^2-44n+265}$$
$$+ 4\sqrt{2}(2n^3-18n^2+52n-48)\Big]$$

$${}^{m}SO(G) = 4\frac{1}{\sqrt{1^2+4^2}} + 12(n-2)\frac{1}{\sqrt{2^2+4^2}} + (6n^2-30n+36)\frac{1}{\sqrt{3^2+4^2}} + \frac{1}{3}(2n^3-18n^2+52n-48)\frac{1}{\sqrt{4^2+4^2}}$$
$$= \frac{1}{6\sqrt{2}}n^3 + \left(\frac{6}{5}-\frac{3}{2\sqrt{2}}\right)n^2 + \left(\frac{6}{\sqrt{5}}-6+\frac{13}{3\sqrt{2}}\right)n + \left(\frac{4}{\sqrt{17}}-\frac{12}{\sqrt{5}}+\frac{36}{5}-\frac{4}{\sqrt{2}}\right)$$

$$SO_3(G) = \sqrt{2}\pi\left[4\left(\frac{1^2+4^2}{1+4}\right) + 12(n-2)\left(\frac{2^2+4^2}{2+4}\right) + (6n^2-30n+36)\left(\frac{3^2+4^2}{3+4}\right) + \frac{1}{3}(2n^3-18n^2+52n-48)\left(\frac{4^2+4^2}{4+4}\right)\right]$$
$$= \sqrt{2}\pi\left[\frac{8n^3}{3} - \frac{18n^2}{7} + \frac{46n}{21} - \frac{64}{35}\right]$$
$$= \frac{\sqrt{2}\pi}{105}[280n^3 - 270n^2 + 230n - 192]$$

$$SO_4(G) = \frac{\pi}{2}\left[4\left(\frac{1^2+4^2}{1+4}\right)^2 + 12(n-2)\left(\frac{2^2+4^2}{2+4}\right)^2\right.$$
$$\left. + (6n^2-30n+36)\left(\frac{3^2+4^2}{3+4}\right)^2 + \frac{1}{3}(2n^3-18n^2+52n-48)\left(\frac{4^2+4^2}{4+4}\right)^2\right]$$
$$= \frac{\pi}{2}\left[\frac{32n^3}{3} - \frac{954n^2}{49} + \frac{4118n}{147} - \frac{63368}{3675}\right]$$
$$= \frac{\pi}{7350}[39200n^3 - 71550n^2 + 102950n - 63368]$$

□

Table 2. The numerical values of Sombor indices for $n \in \{4, 5...18\}$

SO	SO_{red}	SO_{avr}	^{m}SO	SO_3	SO_4
183.824	131.161	60.3235	8.73671	606.263	731.941
380.117	272.612	105.738	16.9271	1235.88	1522.77
681.665	491.271	167.633	28.9317	2198.08	2755.08
1111.09	804.108	247.604	45.4576	3563.95	4529.42
1691.03	1228.09	347.012	67.2120	5404.58	6946.31
2444.11	1780.20	466.940	94.9019	7791.04	10106.3
3392.95	2477.40	608.186	129.234	10794.4	14109.9
4560.19	3336.65	771.316	170.917	14485.8	19057.6
5968.44	4374.94	956.721	220.656	18936.3	25050.0
7640.34	5609.23	1164.67	279.159	24217.0	32187.6
9598.51	7056.49	1395.36	347.133	30399.0	40571.0
11865.6	8733.69	1648.93	425.285	37553.3	50300.6
14464.2	10657.8	1925.46	514.323	45751.0	61477.0
17417.0	12845.8	2225.04	614.953	55063.3	74200.8
20746.5	15314.7	2547.71	727.882	65561.2	88572.4

4. Entropy of Various Sombor Indices

$$ENT_{SO} = log(SO(G)) - \frac{1}{SO(G)} log\Big[\prod_{uv\in E} \alpha^{\alpha}\Big] \tag{4.1}$$

where $\alpha = \sqrt{deg(u)^2 + deg(v)^2}$

$$\begin{aligned}
ENT_{SO} &= log(SO(G)) - \frac{1}{SO(G)} log\Big[4\sqrt{1^2+4^2}^{\sqrt{1^2+4^2}} + 12(n-2)\sqrt{2^2+4^2}^{\sqrt{2^2+4^2}} \\
&+ (6n^2-30n+36)\sqrt{3^2+4^2}^{\sqrt{3^2+4^2}} \\
&+ \frac{1}{3}(2n^3-18n^2+52n-48)\sqrt{4^2+4^2}^{\sqrt{4^2+4^2}}\Big] \\
&= log(3.771n^3-3.941n^2+1.718n-1.349) - \frac{log(1376.244)}{3.771n^3-3.941n^2+1.718n-1.349} \\
&- \frac{log(9735.825(n-2))}{3.771n^3-3.941n^2+1.718n-1.349} - \frac{log(3125(6n^2-30n+36))}{3.771n^3-3.941n^2+1.718n-1.349} \\
&- \frac{log(6026.786(2n^3-18n^2+52n-48))}{3.771n^3-3.941n^2+1.718n-1.349}
\end{aligned}$$

$$
\begin{aligned}
ENT_{SO_{red}} &= log(SO(G)_{red}) - \frac{1}{SO(G)_{red}} log\Bigg[4\sqrt{(1-1)^2+(4-1)^2}^{\sqrt{(1-1)^2+(4-1)^2}} \\
&+ 12(n-2)\sqrt{(2-1)^2+(4-1)^2}^{\sqrt{(2-1)^2+(4-1)^2}} \\
&+ (6n^2-30n+36)\sqrt{(3-1)^2+(4-1)^2}^{\sqrt{(3-1)^2+(4-1)^2}} \\
&+ \frac{1}{3}(2n^3-18n^2+52n-48)\sqrt{(4-1)^2+(4-1)^2}^{\sqrt{(4-1)^2+(4-1)^2}}\Bigg] \\
&= log(2.828n^3-3.823n^2-3.320n-1.977) - \frac{log(108)}{2.828n^3-3.823n^2-3.320n-1.977} \\
&- \frac{log(457.425(n-2))}{2.828n^3-3.823n^2-3.320n-1.977} - \frac{log(101.904(6n^2-30n+36))}{2.828n^3-3.823n^2-3.320n-1.977} \\
&- \frac{log(153.361(2n^3-18n^2+52n-48))}{2.828n^3-3.823n^2-3.320n-1.977}
\end{aligned}
$$

$$
\begin{aligned}
ENT_{SO_{avr}} &= log(SO_{avr}(G)) - \frac{1}{SO(G)_{avr}} log\Bigg[4\sqrt{(1-r)^2+(4-r)^2}^{\sqrt{(1-r)^2+(4-r)^2}} \\
&+ 12(n-2)\sqrt{(2-r)^2+(4-r)^2}^{\sqrt{(2-r)^2+(4-r)^2}} \\
&+ (6n^2-30n+36)\sqrt{(3-r)^2+(4-r)^2}^{\sqrt{(3-r)^2+(4-r)^2}} \\
&+ \frac{1}{3}(2n^3-18n^2+52n-48)\sqrt{(4-r)^2+(4-r)^2}^{\sqrt{(4-r)^2+(4-r)^2}}\Bigg]
\end{aligned}
$$

where $SO_{avr}(G) = \frac{1}{(2n+1)}\Big[4\sqrt{36n^2-108n+225} + 24(n-2)\sqrt{4n^2-20n+61} + (6n^2-30n+36)\sqrt{4n^2-44n+265} + 4\sqrt{2}(2n^3-18n^2+52n-48)\Big]$ and $r = \frac{8(n^2-1)}{(n+1)(2n+1)}$.

$$
\begin{aligned}
ENT_{^mSO} &= log(^mSO(G)) - \frac{1}{^mSO(G)} log\Bigg[4\left(\frac{1}{\sqrt{1^2+4^2}}\right)^{\frac{1}{\sqrt{1^2+4^2}}} + 12(n-2)\left(\frac{1}{\sqrt{2^2+4^2}}\right)^{\frac{1}{\sqrt{2^2+4^2}}} \\
&+ (6n^2-30n+36)\left(\frac{1}{\sqrt{3^2+4^2}}\right)^{\frac{1}{\sqrt{3^2+4^2}}} + \frac{1}{3}(2n^3-18n^2+52n-48)\left(\frac{1}{\sqrt{4^2+4^2}}\right)^{\frac{1}{\sqrt{4^2+4^2}}}\Bigg] \\
&= log(0.118n^3+0.139n^2-0.253n-0.025) - \frac{log(2.837)}{0.118n^3+0.139n^2-0.253n-0.025} \\
&- \frac{log(8.585(n-2))}{0.118n^3+0.139n^2-0.253n-0.025} - \frac{log(0.725(6n^2-30n+36))}{0.118n^3+0.139n^2-0.253n-0.025} \\
&- \frac{log(0.245(2n^3-18n^2+52n-48))}{0.118n^3+0.139n^2-0.253n-0.025}
\end{aligned}
$$

$$
\begin{aligned}
ENT_{SO_3} &= log(SO_3(G)) - \frac{1}{SO_3(G)} log\Bigg[4\sqrt{2}\pi\left(\frac{1^2+4^2}{1+4}\right)^{\sqrt{2}\pi\left(\frac{1^2+4^2}{1+4}\right)} + 12(n-2)\sqrt{2}\pi\left(\frac{2^2+4^2}{2+4}\right)^{\sqrt{2}\pi\left(\frac{2^2+4^2}{2+4}\right)} \\
&+ (6n^2-30n+36)\sqrt{2}\pi\left(\frac{3^2+4^2}{3+4}\right)^{\sqrt{2}\pi\left(\frac{3^2+4^2}{3+4}\right)} + \frac{1}{3}(2n^3-18n^2+52n-48)\sqrt{2}\pi\left(\frac{4^2+4^2}{4+4}\right)^{\sqrt{2}\pi\left(\frac{4^2+4^2}{4+4}\right)}\Bigg] \\
&= log(11.842n^3 - 11.419n^2 + 9.727n - 8.120) - \frac{log(6.303\times 10^{17})}{11.842n^3 - 11.419n^2 + 9.727n - 8.120} \\
&- \frac{log(2.525\times 10^{18}(n-2))}{11.842n^3 - 11.419n^2 + 9.727n - 8.120} - \frac{log(1.085\times 10^{19}(6n^2-30n+36))}{11.842n^3 - 11.419n^2 + 9.727n - 8.120} \\
&- \frac{log(1.564\times 10^{22}(2n^3-18n^2+52n-48))}{11.842n^3 - 11.419n^2 + 9.727n - 8.120}
\end{aligned}
$$

$$
\begin{aligned}
ENT_{SO_4} &= log(SO_4(G)) - \frac{1}{SO_4(G)} log\Bigg[4\left(\frac{\pi}{2}\left(\frac{1^2+4^2}{1+4}\right)^2\right)^{\frac{\pi}{2}\left(\frac{1^2+4^2}{1+4}\right)^2} + 12(n-2)\left(\frac{\pi}{2}\left(\frac{2^2+4^2}{2+4}\right)^2\right)^{\frac{\pi}{2}\left(\frac{2^2+4^2}{2+4}\right)^2} \\
&+ (6n^2-30n+36)\left(\frac{\pi}{2}\left(\frac{3^2+4^2}{3+4}\right)^2\right)^{\frac{\pi}{2}\left(\frac{3^2+4^2}{3+4}\right)^2} + \frac{1}{3}(2n^3-18n^2+52n-48)\left(\frac{\pi}{2}\left(\frac{4^2+4^2}{4+4}\right)^2\right)^{\frac{\pi}{2}\left(\frac{4^2+4^2}{4+4}\right)^2}\Bigg] \\
&= log(16.747n^3 - 30.567n^2 + 43.981n - 27.071) - \frac{log(2.814\times 10^{23})}{16.747n^3 - 30.567n^2 + 43.981n - 27.071} \\
&- \frac{log(5.478\times 10^{22}(n-2))}{16.747n^3 - 30.567n^2 + 43.981n - 27.071} - \frac{log(1.161\times 10^{26}(6n^2-30n+36))}{16.747n^3 - 30.567n^2 + 43.981n - 27.071} \\
&- \frac{log(4.913\times 10^{34}(2n^3-18n^2+52n-48))}{16.747n^3 - 30.567n^2 + 43.981n - 27.071}
\end{aligned}
$$

Table 3. The numerical values of Sombor entropies for $n \in \{5, 6...18\}$

SO	SO_{red}	SO_{avr}	^mSO	SO_3	SO_4
8.41713	7.73641	6.57981	3.34660	10.0540	10.3316
9.32245	8.72212	7.27761	4.30731	10.9780	11.2932
10.0601	9.50475	7.86114	5.10628	11.7218	12.0624
10.6847	10.1577	8.36717	5.77296	12.3483	12.7076
11.2274	10.7198	8.80985	6.34199	12.8914	13.2652
11.7080	11.2143	9.20189	6.83805	13.3715	13.7571
12.1395	11.6562	9.55281	7.27805	13.8024	14.1976
12.5312	12.0561	9.86981	7.67377	14.1934	14.5967
12.8900	12.4213	10.1584	8.03365	14.5514	14.9617
13.2210	12.7576	10.4230	8.36392	14.8818	15.2981
13.5282	13.0692	10.6669	8.66928	15.1884	15.6100
13.8150	13.3597	10.8931	8.95339	15.4746	15.9009
14.0838	13.6316	11.1038	9.21912	15.7430	16.1733
14.3369	13.8873	11.3009	9.46881	15.9955	16.4295

5. Graphical comparison

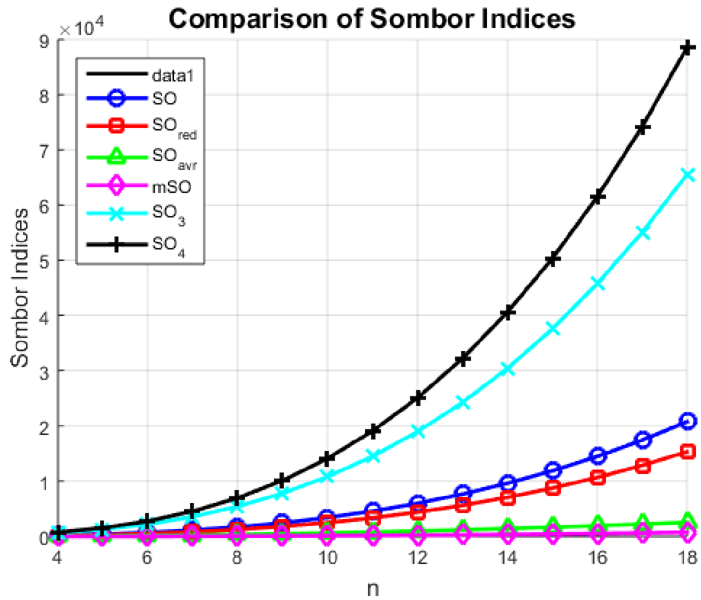

Figure 6. Graphical trends of various Sombor indices for the tetrahedral diamond lattice $TD(n)$, where $n \in \{4, 5, \ldots, 18\}$.

To place our results in the context of existing research, we present a graphical comparison of the Sombor indices computed for the tetrahedral diamond lattice $TD(n)$, where n denotes the number of layers. Although several studies have focused on two-dimensional molecular graphs, such as hexagonal lattices, benzenoids, and graphene, the extension of these investigations to three-dimensional nanostructures remains limited.

Shanmukha et al. [11] studied the expected values of Sombor indices and their entropy measures for graphene, a planar carbon structure with hexagonal symmetry. Their work showed sub-cubic growth trends in classical and modified Sombor indices. Similarly, Ramane et al. [10] analyzed a wide range of molecular structures, including fullerenes and benzenoids, and observed predominantly quadratic growth patterns for these indices.

In contrast, our analytical expressions for $TD(n)$ reveal significantly different behavior. Specifically, indices such as SO, SO_3, and SO_4 demonstrate cubic growth with respect to n, as evidenced by the leading n^3 terms in their closed-form formulas. This reflects the higher complexity and denser connectivity in the three-dimensional tetrahedral diamond lattice compared to planar graphs.

Figure 6 illustrates the numerical growth of six Sombor indices, SO, SO_{red}, SO_{avr}, ${}^{m}SO$, SO_3, and SO_4, over the range $n = 4$ to 18. See Table 2. The steep curves for SO_3 and SO_4 in particular highlight the influence of higher-degree vertex combinations in the 3D lattice. This graphical trend supports the theoretical expressions and emphasizes the structural richness of $TD(n)$.

Furthermore, Table 3 presents the entropy values corresponding to each of the six Sombor indices. Compared to the entropy measures reported in [11] for planar molecular structures, our results exhibit consistently higher entropy values. This reflects the greater topological irregularity and information density inherent in the tetrahedral diamond lattice $TD(n)$. Such behavior underscores the effectiveness of entropy-based indices in distinguishing the structural complexity of molecular graphs.

Figure 7 provides a visual comparison of these entropy trends. The combined numerical and graphical evidence confirms that Sombor indices and their entropy variants are valuable tools for quantifying and interpreting the intricate topology of three-dimensional nanostructures.

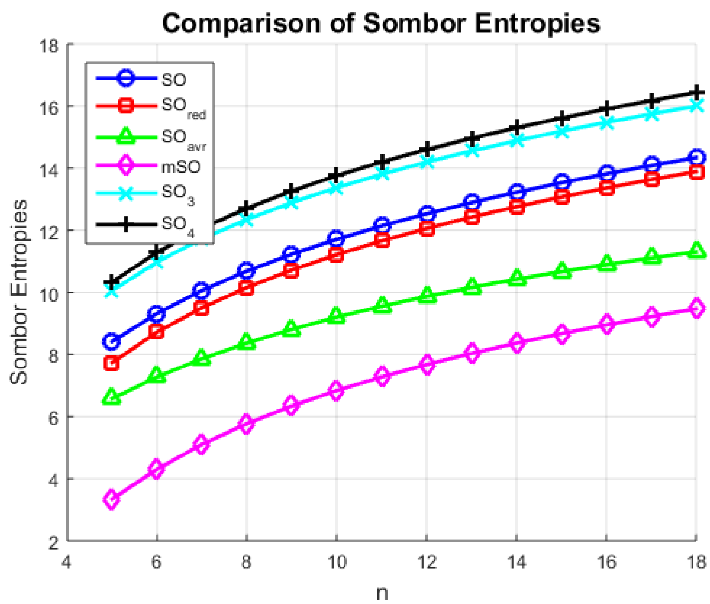

Figure 7. Entropy trends of various Sombor indices for the tetrahedral diamond lattice $TD(n)$, where $n \in \{5, 6, \ldots, 18\}$.

6. Conclusion

Carbon is a significant constituent of the chemical system, creating a wide range of compounds due to its small size and strong chemical bonding capabilities. Diamond possesses significant potential for utilisation in a wide range of industrial and commercial applications owing to its diverse and exceptional properties. Analytical expressions for Sombor indices and associated entropy measurements for the graph of tetrahedral diamond lattices have been calculated precisely. These numerical expressions offer vital insights into the topological characteristics of the graph representing the tetrahedral diamond lattice.

Acknowledgment. This research work is supported by SRM Institute of Science and Technology under Selective Excellence Research Initiative 2023.

Conflicts of Interest: The authors declare that there are no conflicts of interest regarding the publication of this paper.

References

[1] K.C. Das, I. Gutman, B. Furtula, On Atom-Bond Connectivity Index, Filomat 26 (2012), 733–738. https://doi.org/10.2298/FIL1204733D.

[2] M. Dehmer, A. Mowshowitz, A History of Graph Entropy Measures, Inf. Sci. 181 (2011), 57–78. https://doi.org/10.1016/j.ins.2010.08.041.

[3] I. Gutman, N. Trinajstić, Graph Theory and Molecular Orbitals. Total φ-Electron Energy of Alternant Hydrocarbons, Chem. Phys. Lett. 17 (1972), 535–538. https://doi.org/10.1016/0009-2614(72)85099-1.

[4] I. Gutman, Molecular Graphs With Minimal and Maximal Randić Indices, Croat. Chem. Acta 75 (2002), 357–369.

[5] I. Gutman, Degree-Based Topological Indices, Croat. Chem. Acta 86 (2013), 351–361. https://doi.org/10.5562/cca2294.

[6] I. Gutman, Geometric Approach to Degree-Based Topological Indices: Sombor Indices, MATCH Commun. Math. Comput. Chem. 86 (2021), 11–16.

[7] H. Hosoya, Topological Index. A Newly Proposed Quantity Characterizing the Topological Nature of Structural Isomers of Saturated Hydrocarbons, Bull. Chem. Soc. Jpn. 44 (1971), 2332–2339. https://doi.org/10.1246/bcsj.44.2332.

[8] V.R. Kulli, Sombor Indices of Certain Graph Operators, Int. J. Eng. Sci. Res. Technol. 10 (2021), 127–134. https://doi.org/10.29121/ijesrt.v10.i1.2021.12.

[9] P. Manuel, B. Rajan, C. Grigorious, S. Stephen, On the Strong Metric Dimension of Tetrahedral Diamond Lattice, Math. Comput. Sci. 9 (2015), 201–208. https://doi.org/10.1007/s11786-015-0226-0.

[10] H.S. Ramane, I. Gutman, K. Bhajantri, D.V. Kitturmath, Sombor Index of Some Graph Transformations, Commun. Comb. Optim. 8 (2023), 193–205. https://doi.org/10.22049/cco.2021.27484.1272.

[11] M.C. Shanmukha, K.J. Gowtham, A. Usha, K. Julietraja, Expected Values of Sombor Indices and Their Entropy Measures for Graphene, Mol. Phys. 122 (2023), e2276905. https://doi.org/10.1080/00268976.2023.2276905.

[12] C.E. Shannon, A Mathematical Theory of Communication, Bell Syst. Tech. J. 27 (1948), 379–423. https://doi.org/10.1002/j.1538-7305.1948.tb01338.x.